INVESTIGATION OF ASYMMETRIC EDGE DIFFRACTION FOR ACOUSTIC BARRIERS

Mihai BUGARU[1], Marian NEAGOE[2]

The paper aims to investigate asymmetric edge diffraction for acoustic barriers designed for automotive and railway traffic noise attenuation. For this purpose, it was used the Modified General Prediction Method (MGPM) is already in use for the estimation of industrial noise. If MGPM gives satisfactory results for reducing industrial noise, it can also be used to estimate noise reduction if the noise pollution is caused by automotive and railway traffic. Based on this aspect, some geometrical aspects of asymmetric edge diffraction were optimized. The predicted values were compared with experimental data in the literature, and agreement was found.

Keywords: edge diffraction, acoustic barriers, noise attenuation

1. Introduction

The present paper presents a detailed investigation of an asymmetric edge diffraction mounted on a rigid acoustic barrier designed for automotive and railway traffic noise attenuation. The study comprises the optimization of the asymmetric edge diffraction using the Modified General Prediction Method (MGPM) developed by the authors in previous research[1]. The MGPM can be applied directly for symmetric edge diffraction (see Fig. 1) but must be modified for asymmetric edge diffraction. In general, asymmetric edge diffraction is used for attenuating industrial noise, as mentioned by Okubo and Fujiwara in [2], but the authors of the paper analysis also the possibilities of using such types of edge diffraction for automotive and railway traffic noise attenuation(AARTNA).

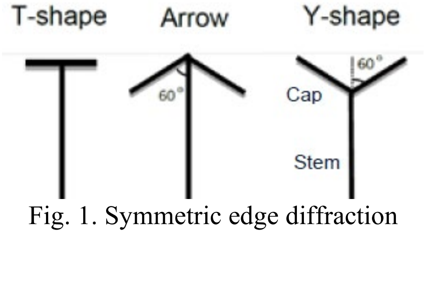

Fig. 1. Symmetric edge diffraction

[1] Prof., Dept. of Mechanics, University POLITEHNICA of Bucharest, Romania,
e-mail:skmbugaru@yahoo.com
[2] Eng., Authority of Regional Roads-Valcea, Romania, e-mail: neagoe_florin_marian@yahoo.com

The MGPM [1] is a modified version of the general prediction method (GPM), the GPM being presented in detail in the standard ISO-9613[3]. The noise attenuation of the barrier, enhancing the GPM, is computed based on the Kirchhoff diffraction theory, which implies that the Huygens-Fresnel theory is applied to a semi-infinite acoustic thin, rigid barrier (SIATRB). The Maekawa-Tatge algorithm[4,5] and Kurze&Anderson model[6] realize similar data since they compute the noise attenuation using the Fresnel number N_1. This aspect involves the phenomenon of "*the effect of the relative position of the receiver from the source"*[1]. The GPM includes two phenomena: "*the impact of the relative position of the receiver from the source* and *the downwind meteorological effect"*[1].

As mentioned in the paper [1], "the best-predicting method for noise attenuation prediction in the case of a thin, rigid semi-infinite acoustic barrier is the MGPM"[1], already certified by the experimental data published in the literature [7,8]. The MGPM is an improvement of GPM by inducing new acoustical effects, such as "*the proximity of the source or the receiver to the midplane attenuation due to geometrical divergence"*[1,9], "*ground absorption-reflections"*(GAR)[1,10], and "*atmospheric absorption"*(AA)[1,11,12]. This research aimed to provide a modified version of MGPM for asymmetric edge diffraction (AED) mounted on a SIATRB designed for AARTNA.

2. The modified version of MGPM enhanced for AED

Figure 2 illustrates an SIATRB with the height H, an acoustic source (AS) with the coordinates $(0, y_S)$, an acoustic receiver (AR) with the coordinates $(x_R + x_S, y_R)$, and an AED with the geometry details.

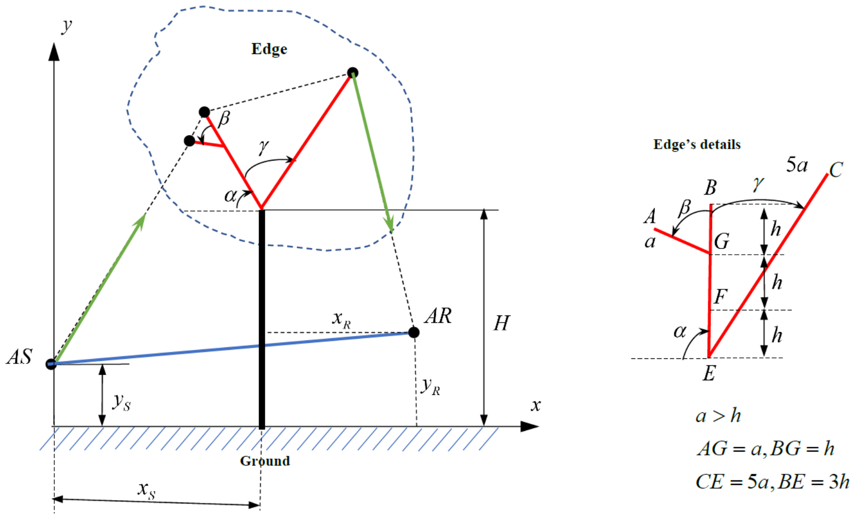

Fig. 2. An SIATRB with an AED mounted on the top.

The MGPM considers the attenuation introduced by ground absorption reflections, and for this, the most convenient model is the Delany-Bazley model [10], resulting in the modified wavenumber k_{mod} due to "*the effect of ground absorption*"[1]

$$k_{mod} = \frac{2\pi f}{c\left[1+0.0978\left[\frac{f}{\sigma_e}\right]^{-0.7} - i0.189\left[\frac{f}{\sigma_e}\right]^{-0.595}\right]}, i=\sqrt{-1}, \tag{1}$$

where f is "*the pure tone frequency*"(PTF)[1], σ_e is "*the effective flow resistivity of the ground*"(EFRG)[1,10], and c is "*the sound speed in the air*"(SSA)[1]. Based on the Kirchhoff-Fresnel diffraction theory [13](pp. 113–147), the Fresnel numbers of the AS and the image of the AS, respectively AS' (the symmetric geometric point concerning the plane of the barrier) are N_1, N_2, given by the relations

$$N_1 = \frac{2\delta_1 f}{c} = \frac{k_{mod}}{\pi}\delta_1, N_2 = \frac{2\delta_2 f}{c} = \frac{k_{mod}}{\pi}\delta_2, \tag{2}$$

where δ_1, δ_2 are the distances defined by the longest propagation way of the acoustic wave and the shortest one, respectively (AS $\rightarrow$A $\rightarrow$B $\rightarrow$C $\rightarrow$AR) - (AS $\rightarrow$AR), and (AS $\rightarrow$A $\rightarrow$B $\rightarrow$C $\rightarrow$AR) - (AS' $\rightarrow$AR), defined by the expressions

$$\begin{aligned}
&\delta_1 = r_1 + r_2 + r_3 + r_4 - \sqrt{(x_S + x_R)^2 + (y_R - y_S)^2} = r_1 + r_2 + r_3 + r_4 - d_1,\\
&r_1 = \sqrt{(0 - x_A)^2 + (y_S - y_A)^2}, r_2 = \sqrt{(x_B - x_A)^2 + (y_B - y_A)^2},\\
&r_3 = \sqrt{(x_C - x_B)^2 + (y_C - y_B)^2}, r_4 = \sqrt{(x_R + x_S - x_C)^2 + (y_R - y_C)^2},\\
&x_A = x_S - 2h\cos\alpha - a\cos(\alpha - \beta) = a\left(x_S / a - 2\varsigma\cos\alpha - \cos(\alpha-\beta)\right), \varsigma = h/a, \varsigma = 0.5 - 0.9,\\
&y_A = y_E + 2h\sin\alpha + a\sin(\alpha-\beta) = a\left(H/a + 2\varsigma\sin\alpha + \sin(\alpha-\beta)\right), y_E = H,\\
&x_B = x_S - 3h\cos\alpha = a\left(x_S/a - 3\varsigma\cos\alpha\right), y_B = y_E + 3h\sin\alpha = a\left(H/a + 3\varsigma\sin\alpha\right),\\
&x_C = x_S - 5a\cos(\alpha+\gamma) = a\left(x_S/a - 5\cos(\alpha+\gamma)\right), y_C = y_E + 5a\sin(\alpha+\gamma) = a\left(H/a + 5\sin(\alpha+\gamma)\right),\\
&\delta_2 = r_1 + r_2 + r_3 + r_4 - \sqrt{(x_R - x_S)^2 + (y_R - y_S)^2} = r_1 + r_2 + r_3 + r_4 - d_2, x_R > x_S, y_R > y_S,
\end{aligned} \tag{3}$$

where d_1 is the distance between the points AS and AR(respectively (AS$\rightarrow$AR)), while d_2 is the distance between the points AS' and AR(respectively (AS'$\rightarrow$AR)).

Because the GPM [5,6] provides a relation for the sound attenuation based on a modified Fresnel number N_1' as mentioned in ISO 9613-2 [3], taking into consideration a correction factor for the downwind meteorological effect $Kmet$, the MGPM considers the same correction factor thus, yielding the relations

$$K_{met} = exp\left(-\frac{1}{2000}\sqrt[4]{\frac{r_1 r_2 r_3 r_4 d_1}{2\delta_1}} \right), N_1' = 0.5 N_1 K_{met}. \quad (4)$$

The MGPM also considers(see [1]) the AA using the Larsson model [11], which induces in the predictive model the following effects: sound frequency, air humidity, air temperature, and pressure, using an attenuation coefficient α_{aa}, expressed in dBA/m, described by the relation

$$\alpha_{aa} = f^2 \left[\left[\left(\frac{1.84x10^{-11}}{\left(\frac{T_0}{T} \right)^{0.5} \frac{p_s}{p_0}} \right) + \left(\frac{T_0}{T} \right)^{2.5} \left(\frac{0.1068 e^{-3352/T} f_{r,N}}{f^2 + f_{r,N}^2} + \frac{0.01278 e^{-2239.1/T} f_{r,O}}{f^2 + f_{r,O}^2} \right) \right] \right], \quad (5)$$

where the significations of the terms are explained in detail in [11,12].

Considering all the aspects mentioned above, expressed by the relations (1)-(5), the sound attenuation proposed by MGPM [1] when using an SIATRB for AARTNA with an AED is given by the equation

$$A_{MGPM} = 10 log_{10}\left(3 + 20N_1'\right) + \alpha_{aa}(r_1 + r_2 + r_3 + r_4) +$$
$$+ \left[6 tanh\sqrt{N_2} - 2 - 20 log_{10}\left[1 + tanh\left(0.6 log_{10}\frac{N_2}{N_1'} \right) \right] \right] \left[1 - tanh\sqrt{10N_1'} \right]. \text{ [dB]} \quad (6)$$

To have the diffractions directions that induce the sound attenuation in conformity with the mathematical algorithm generated by the expressions (1)-(6), it is necessary to impose certain simultaneous geometrical restrictions as follows

1. point A must be “over” the direction line AS$\rightarrow$B,
2. point C must be “over” the direction line B$\rightarrow$AR,
3. $h < a, h / a = \varsigma \in \left[0.5, 0.9\right]$.

Condition 2, for an existing condition three true, is satisfied if

$$\alpha + \gamma \leq \pi , \quad (7)$$

while condition 1 is satisfied for

$$\beta \leq \beta_{max} = \pi - \phi - arcsin\left(\varsigma sin\phi\right), \phi = arccos\left[\frac{x_B^2 + \left(y_B - y_S\right)^2 + 9\left(a\varsigma\right)^2 - x_S^2 - \left(H - y_S\right)^2}{6a\varsigma\sqrt{x_B^2 + \left(y_B - y_S\right)^2}} \right]. \quad (8)$$

Condition 3, together with relations (7) and (8) and the expressions of the coordinates, $x_A, y_A, x_B, y_B, x_C, y_C$ define from a geometrical point of view the existence of an asymmetric edge diffraction(AED) for an SIATRB designed to obtain a convenient AARTNA. The aspects mentioned before are valid for the angles α, β, γ satisfying the conditions

$$\alpha \in \left[1^0, 179^0 - \phi_1\right], \phi_1 = arct\,g\frac{H - y_S}{x_S}, \quad (9)$$

$$\beta \in \left[1^0, \beta_{max}\right], \beta_{max} \Leftarrow (8), \tag{10}$$

$$\gamma \in \left[1^0, \gamma_{max}\right], \gamma_{max} = 1^0 + arctg\frac{H - y_S}{x_S}, \tag{11}$$

and the attenuation is computed using the algorithm given by equations (1)-(6), representing the first part of the investigation. The second part of the investigation the angles α, β, γ satisfy the conditions

$$\alpha \in \left[180^0 - \phi_1, 179^0\right], \phi_1 = arctg\frac{H - y_S}{x_S}, \tag{12}$$

$$\beta \in \left[1^0, 179^0\right], \tag{13}$$

$$\gamma \in \left[1^0, arctg\frac{H - y_S}{x_S}\right], \tag{14}$$

but the attenuation is computed in this case by modifying equations (3) and (4) due to modifications of the propagation way for the acoustic wave that are (AS$\rightarrow$E$\rightarrow$A$\rightarrow$B$\rightarrow$C$\rightarrow$AR)-(AS$\rightarrow$AR), respectively (AS$\rightarrow$E$\rightarrow$A$\rightarrow$B$\rightarrow$C$\rightarrow$AR) - (AS' $\rightarrow$AR), defined by the relations

$$\begin{aligned}
&\delta_1 = r_1 + r_2 + r_3 + r_4 + r_5 - \sqrt{(x_S + x_R)^2 + (y_R - y_S)^2} = r_1 + r_2 + r_3 + r_4 + r_5 - d_1,\\
&r_1 = \sqrt{(x_S)^2 + (H - y_S)^2}, r_2 = \sqrt{(x_A - x_S)^2 + (y_A - H + y_S)^2}, r_3 = \sqrt{(x_B - x_A)^2 + (y_B - y_A)^2},\\
&r_4 = \sqrt{(x_C - x_B)^2 + (y_C - y_B)^2}, r_5 = \sqrt{(x_R + x_S - x_C)^2 + (y_R - y_C)^2},\\
&x_A = x_S - 2h\cos\alpha - a\cos(\alpha - \beta) = a\left(x_S / a - 2\varsigma\cos\alpha - \cos(\alpha - \beta)\right), \varsigma = h / a, \varsigma = 0.5 - 0.9,\\
&y_A = H + 2h\sin\alpha + a\sin(\alpha - \beta) = a\left(H / a + 2\varsigma\sin\alpha + \sin(\alpha - \beta)\right),\\
&x_B = x_S - 3h\cos\alpha = a\left(x_S / a - 3\varsigma\cos\alpha\right), y_B = y_E + 3h\sin\alpha = a\left(H / a + 3\varsigma\sin\alpha\right), y_E = H,\\
&x_C = x_S - 5a\cos(\alpha + \gamma) = a\left(x_S / a - 5\cos(\alpha + \gamma)\right), y_C = y_E + 5a\sin(\alpha + \gamma) = a\left(H / a + 5\sin(\alpha + \gamma)\right),\\
&\delta_2 = r_1 + r_2 + r_3 + r_4 + r_5 - \sqrt{(x_R - x_S)^2 + (y_R - y_S)^2} = r_1 + r_2 + r_3 + r_4 + r_5 - d_2, x_R > x_S, y_R > y_S,
\end{aligned} \tag{15}$$

where d_1, d_2 has the same significations as for relation (3), and the modified Fresnel number N_1', as mentioned in ISO 9613-2 [3], taking into consideration the correction factor for the downwind meteorological effect $Kmet$, is defined by the equations

$$K_{met} = exp\left(-\frac{1}{2000}\sqrt[5]{\frac{r_1 r_2 r_3 r_4 r_5 d_1}{2\delta_1}}\right), N_1' = 0.5 N_1 K_{met}. \quad (16)$$

In this second case, the sound attenuation proposed by MGPM [1] when using an SIATRB for AARTNA with an AED is given by the equation

$$A_{MGPM} = 10 log_{10}\left(3 + 20N_1'\right) + \alpha_{aa}\left(r_1 + r_2 + r_3 + r_4 + r_5\right) + \\ + \left[6 tanh\sqrt{N_2} - 2 - 20 log_{10}\left[1 + tanh\left(0.6 log_{10}\frac{N_2}{N_1'}\right)\right]\right]\left[1 - tanh\sqrt{10N_1'}\right], \text{[dB]} \quad (17)$$

where N_1' is determined using equations (1), (2), (15), (16), and for the last equation, in addition, is used equation (5). It can be concluded that the mathematical algorithm in the second case to compute the AARTNA using an SIATRB with an AED is given by the equations (1), (2), (5), (15)-(17).

3. Optimization of the AED

Figure 2 illustrates an AED mounted on the top of the SIATRB designed for AARTNA, and the geometrical data characteristics of the AED and the SIATRB are mentioned in Table 1, while the angles α, β, and γ are variable and need to be optimized.

Table 1

Geometrical details of the AED and the SIATRB

H [m]	x_S [m]	y_S [m]	x_R [m]	y_R [m]	a [m]	$\varsigma = h / a$
4	3.0	0.4	2.0…50.0	1.5	0.20	0.5…0.9

Using equations (1)-(6), for the first case defined by the conditions (9)-(11), and the equations (1), (2), (5), (15)-(17), for the second case defined by the conditions (12)-(14), it was developed MATLAB software to calculate the AARTNA for the SIATRB with AED.

Figures 3-6 illustrate the noise attenuation for the first case considering $x_R = 25.0$ m, the sound's PTF $f = 1.0$ kHz, the EFRG $\sigma_e = 1.0 \cdot 10^5$ Pa·s·m^{-2}, $\varsigma = 0.5, 0.9$ and the angles range $\alpha \in \left[1^0, 129^0\right], \gamma \in \left[1^0, 51^0\right], \beta \in \left[1^0, \beta_{max}\right]$ (for β_{max} see (8)).

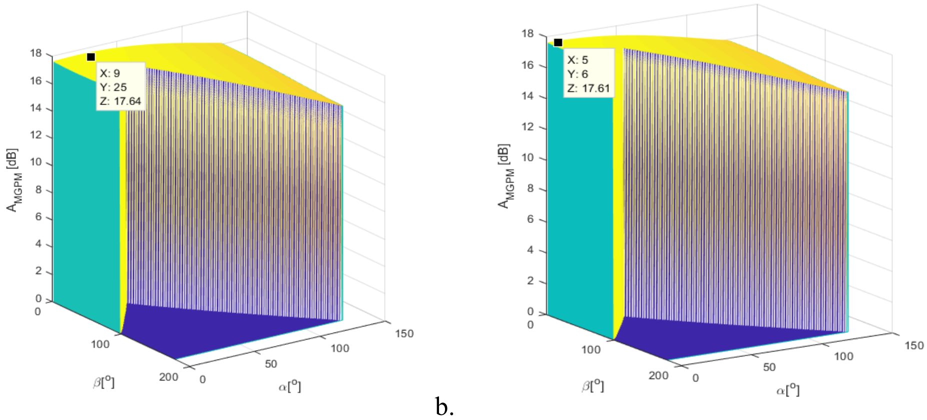

a. b.

Fig. 3. Noise attenuation for PTF $f = 1.0$ kHz, $\varsigma = 0.5$, a. $\gamma = 10^0$, b. $\gamma = 20^0$.

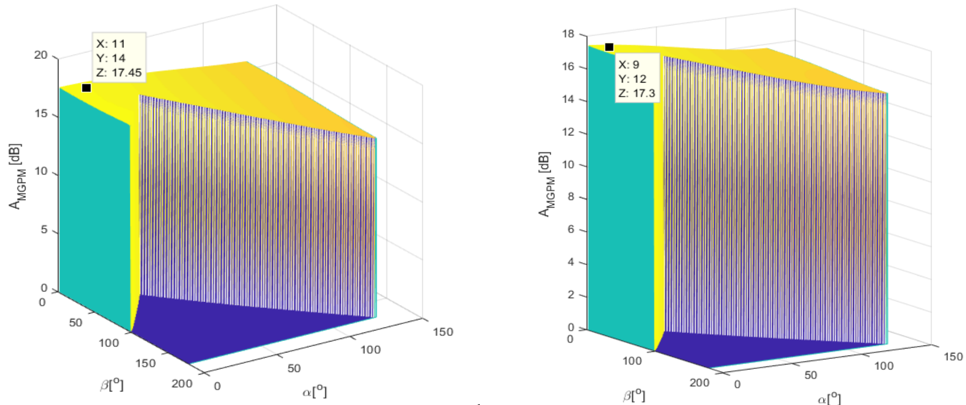

a. b.

Fig. 4. Noise attenuation for PTF $f = 1.0$ kHz, $\varsigma = 0.5$, a. $\gamma = 35^0$, b. $\gamma = 50^0$.

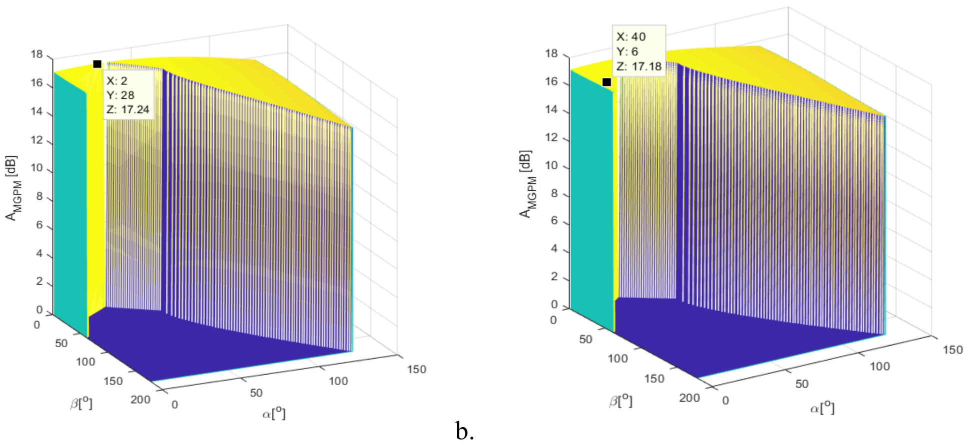

a. b.

Fig. 5. Noise attenuation for PTF $f = 1.0$ kHz, $\varsigma = 0.9$, a. $\gamma = 10^0$, b. $\gamma = 20^0$.

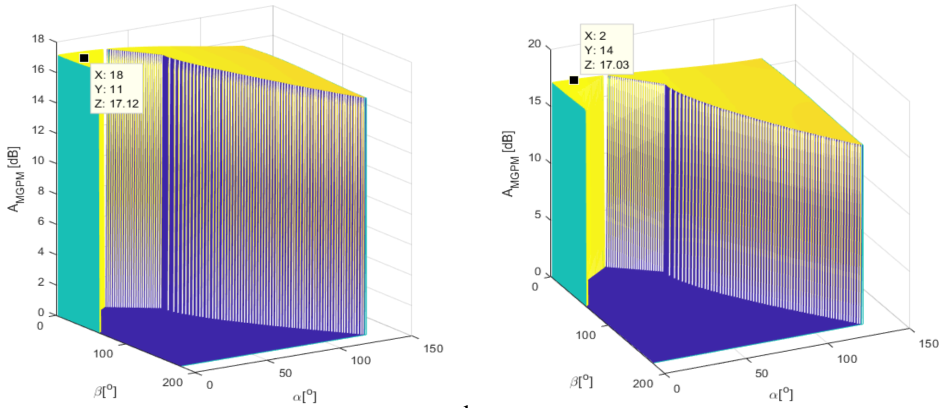

a. b.

Fig. 6. Noise attenuation for PTF $f = 1.0$ kHz, $\varsigma = 0.9$, a. $\gamma = 35^0$, b. $\gamma = 50^0$.

As can be seen from Figures 3-6, for the first case of the investigation, respectively for $x_R = 25.0$ m, the sound's PTF $f = 1.0$ kHz, the EFRG $\sigma_e = 1.0 \cdot 10^5$ Pa·s·m^{-2}, $\varsigma = 0.5, 0.9$ and the angles range $\alpha \in \left[1^0, 129^0\right], \gamma \in \left[1^0, 51^0\right], \beta \in \left[1^0, \beta_{max}\right]$ (for β_{max} see (8)), the maximum attenuation has the value of 17.64 dBA and is obtained for $\varsigma = 0.5$, $\alpha = 25^0, \beta = 9^0, \gamma = 10^0$, (see fig. 3. a.). Analyzing Figures 3-6, it is evident that the ratio $\varsigma = h / a$ has a minor influence on the noise attenuation using an SIATRB with an AED mounted on the top. Figures 7-11 illustrate the noise attenuation for the second case considering $x_R = 25.0$ m, the sound's PTF $f = 1.0$ kHz, the EFRG $\sigma_e = 1.0 \cdot 10^5$ Pa·s·m^{-2}, $\varsigma = 0.5$ and the angles range $\alpha \in \left[130^0, 175^0\right], \gamma \in \left[50^0, 5^0\right], \beta \in \left[1^0, 179^0\right]$, the ratio adopted to minimize the costs.

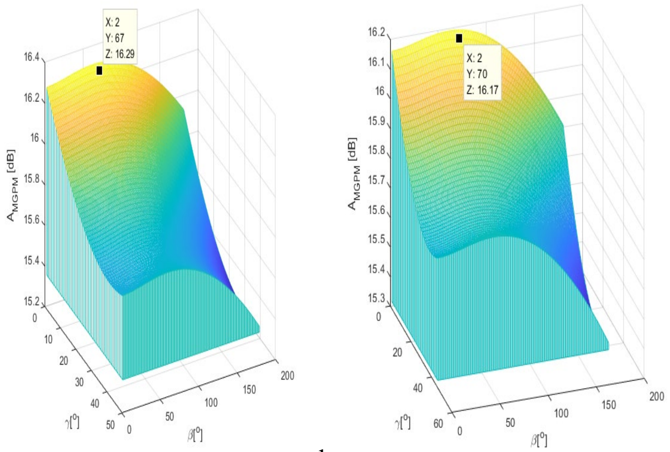

a. b.

Fig. 7. Noise attenuation for PTF $f = 1.0$ kHz, $\varsigma = 0.5$, a. $\alpha = 130^0$, b. $\alpha = 135^0$.

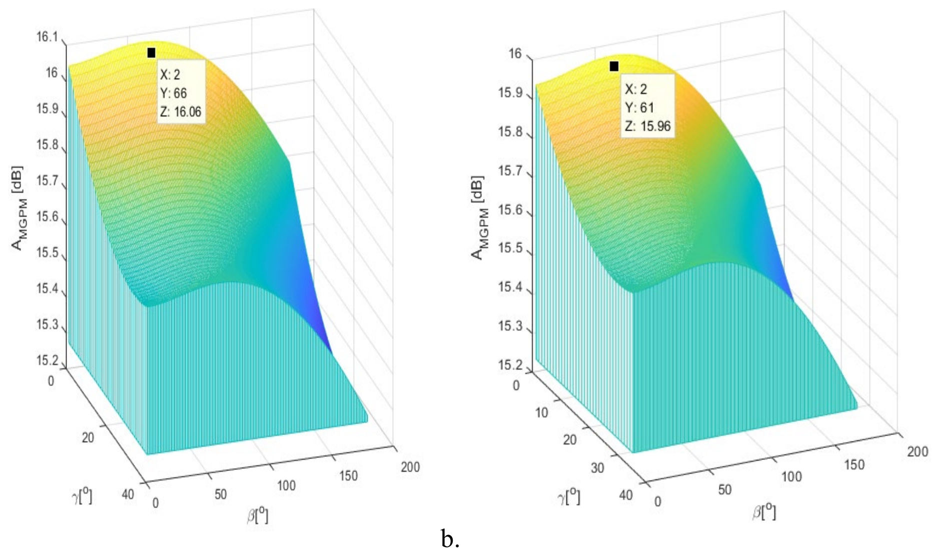

a. b.

Fig. 8. Noise attenuation for PTF $f = 1.0$ kHz, $\varsigma = 0.5$, a. $\alpha = 140^0$, b. $\alpha = 145^0$.

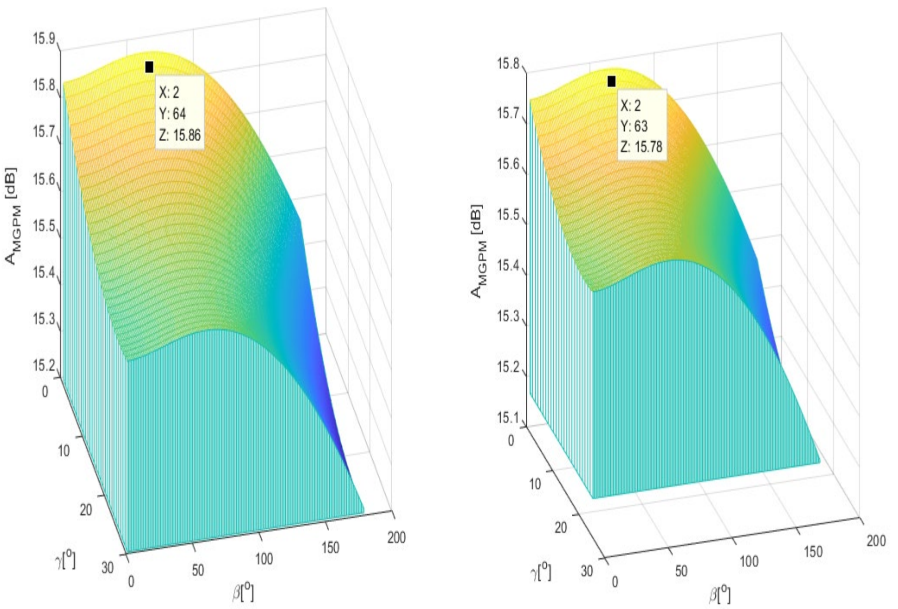

a. b.

Fig. 9. Noise attenuation for PTF $f = 1.0$ kHz, $\varsigma = 0.5$, a. $\alpha = 150^0$, b. $\alpha = 155^0$.

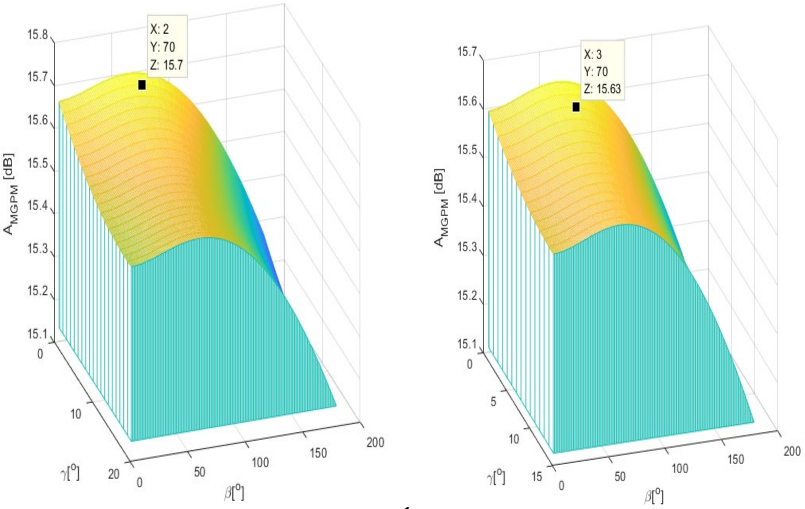

a. b.

Fig. 10. Noise attenuation for PTF $f = 1.0$ kHz, $\varsigma = 0.5$, a. $\alpha = 160^0$, b. $\alpha = 165^0$.

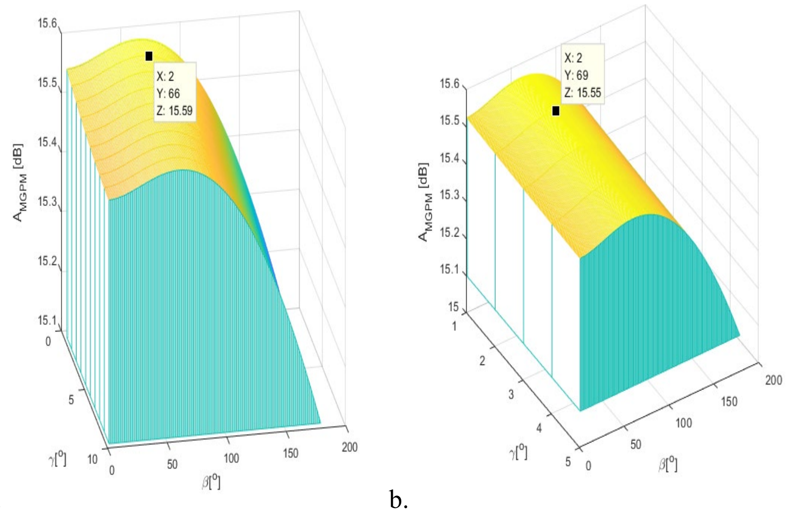

a. b.

Fig. 11. Noise attenuation for PTF $f = 1.0$ kHz, $\varsigma = 0.5$, a. $\alpha = 170^0$, b. $\alpha = 175^0$.

Analyzing Figures 7-11, it is evident that the maximum noise attenuation has the value of 16.29 dBA, which is obtained for the values $\varsigma = 0.5$, $\alpha = 130^0, \beta = 67^0$, $\gamma = 2^0$ (see Figure 7. a.). This noise attenuation value is inferior with more than 1.3 dBA than the maximum value for the first case, which is 17.64 dBA (see Figure 3. a.). Considering the values of the angles, the variation of the noise attenuation, and the practical possibility of realizing such an AED, the optimal geometry to obtain the maximum noise attenuation of at least 17.6 dBA at

25 m distance from the SIATRB for a monopole noise having the PTF f =1.0 kHz is a=0.2 m, h=0.1 m, $\alpha = 25^0, \beta = 9^0, \gamma = 10^0$. The results agree with the data published in the literature[14,15]. Figure 12 illustrates the AARTNA of an SIATRB (having H=4.0 m) with an AED mounted on the top, with geometry characteristics a=0.2 m, h=0.1 m, $\alpha = 25^0, \beta = 9^0, \gamma = 10^0$, for the PTF in the range $f \in [0.1, 3.0]$ kHz and the receiver having the coordinates $x_R \in [0.5, 100.0]$ m, $y_R = 1.5$ m.

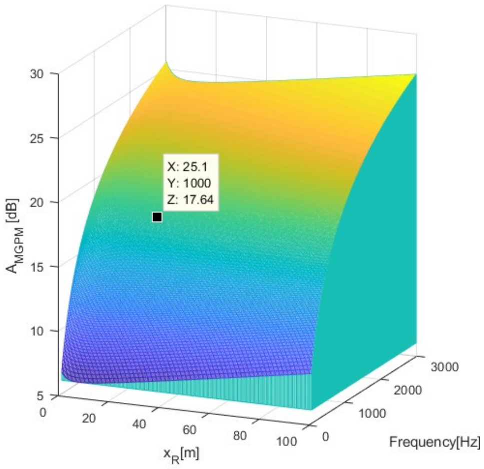

Fig. 12. Noise attenuation for SIATRB with an AED mounted on the top,
$\alpha = 25^0, \beta = 9^0, \gamma = 10^0$, H=4 m, a=0.2 m, h=0.1 m, x_S=3 m, y_S=0.4 m, $x_R \in [0.5, 100.0]$ m, y_R=1.5 m

If we compare the results presented in Fig. 12 with those in the literature [15], it can be remarked the agreement.

4. Conclusions

The investigations carried out on the AED mounted on the top of an SIATRB reveal that the noise attenuation is obtained not only at high frequencies but also at low frequencies showing that this kind of edge diffraction is convenient for AARTNA. Also, the method used for the investigations, respectively the modified version of MGPM, indicates the need to improve ISO standards in the field, more precisely, ISO 96312-2[3]. Another original contribution brought by the paper is using the new concept of *multiple acoustic diffractions* [15] in the optimization theory for AED. Considering a noise attenuation objective of 17.6 dBA at a 25 m distance from the SIATRB for a monopole noise having the PTF f =1.0 kHz for $\varsigma = 0.5$, it yields the angles $\alpha = 25^0, \beta = 9^0, \gamma = 10^0$, using the method designed previously. The results agree with the data published in the literature[14,15]. With the mentioned geometry characteristic data($\varsigma = 0.5$, $\alpha = 25^0, \beta = 9^0, \gamma = 10^0$), the AARTNA of an SIATRB (having H=4.0 m), with an

AED mounted on the top, for the PTF in the range $f \in [0.1, 3.0]$ kHz, is at least 17 dB.

All these previously mentioned aspects and the idea of an international innovation patent to protect MGPM represent the novelty of the present research.

Acknowledgments

This work has been funded by the European Social Fund from the Sectoral Operational Programme Human Capital 2014-2020 through the Financial Agreement with the title "Training of Ph.D. students and postdoctoral researchers in order to acquire applied research skills - SMART", Contract no. 13530/16.06.2022 - SMIS code: 153734.

R E F E R E N C E S

[1]. *M. Bugaru, O. Vasile, M. Neagoe,* "Recent Developments of Noise Attenuation Using Acoustic Barriers for a Specific Edge Geometry", in Computation-MDPI, **vol. 9**, no. 129, Dec. 2021, pp. 1-11

[2]. *T. Okubo, K. Fujiwara*, "Efficient of a noise barrier with an acoustically soft cylindrical edge for practical use", in The Journal of the Acoustical Society of America, **vol. 105**, no. 6, May 1999, pp. 3326-3335

[3]. International Standard Organization. ISO 9613-2: Acoustics: Attenuation of Sound During Propagation Outdoors. Part 2: General Method of Calculation; International Standard Organization: Geneva, Switzerland, 1996

[4]. *Z. Maekawa*, "Noise reduction by screens.", in Applied Acoustics, **vol. 1**, no. 3, July 1968, pp. 157–173

[5]. *R.B. Tatge*, "Barrier-wall attenuation with a finite-sized source", in The Journal of the Acoustical Society of America, **vol. 53**, no. 5, May 1973, pp. 1317–1319

[6]. *U.J. Kurze, G.S. Anderson*, "Sound attenuation by barriers", in Applied Acoustics, **vol. 4**, no. 1, January 1971, pp. 35–53

[7]. *M. Bugaru, M.C. Zaharia, T. Chereches, M. Arsene,* "Multi-layered phono-insulated and phono-absorbing acoustic barrier"-Invention Patent, Official Bulletin of Industrial Property, OSIM, RO-BOPI No. 03/2010, Romanian PATENT no. 122864/2010

[8]. *M. Karimi, D. Younesian*, "Optimized T-Shape and Y-Shape Inclined Sound Barriers for Railway Noise Mitigation", in Journal of Low-Frequency Noise, Vibration, and Active Control, **vol. 33**, no. 3, September 2014, pp. 357–370

[9]. *P. Menounou*, "A correction to Maekawa's curve for the insertion loss behind barriers", in The Journal of the Acoustical Society of America, **vol. 110**, no. 3, November 2001, pp. 1828–1838.

[10]. *M.E. Delany, E.N. Bazley*, "Acoustical properties of fibrous absorbent materials", in Applied Acoustics, **vol. 3**, no. 2, April 1970, pp. 105–116

[11]. *C. Larsson*, "Atmospheric Absorption Conditions for Horizontal Sound Propagation", in Applied Acoustics, **vol. 50**, no. 3, March 1997, pp. 231–245

[12]. International Standard Organization. ISO 9613-1: Acoustics: Noise Absorption by Air. Attenuation of Sound during Propagation Outdoors. Part 2: Calculation of the Absorption of Sound by the Atmosphere, International Standard Organization: Geneva, Switzerland, 1993

[13]. *T.D. Rossing*, Springer Handbook of Acoustics, Springer Science: New York, NY, USA, Würzburg, Germany, 2007.

[14]. *T. Ishizuka, K. Fujiwara*, "Performance of noise barriers with various edge shapes and acoustical conditions", in Applied Acoustics, **vol. 65**, no. 2, February 2004, pp. 125-141

[15]. *D. Pardo-Quiles, J.V. Rodriguez,* "A Fast UTD-Based Method for the Analysis of Multiple Acoustic Diffraction over a Series of Obstacles with Arbitrary Modeling, Height and Spacing", in Symmetry-MDPI, **vol. 12**, no. 654, April 2020, pp. 1-24.